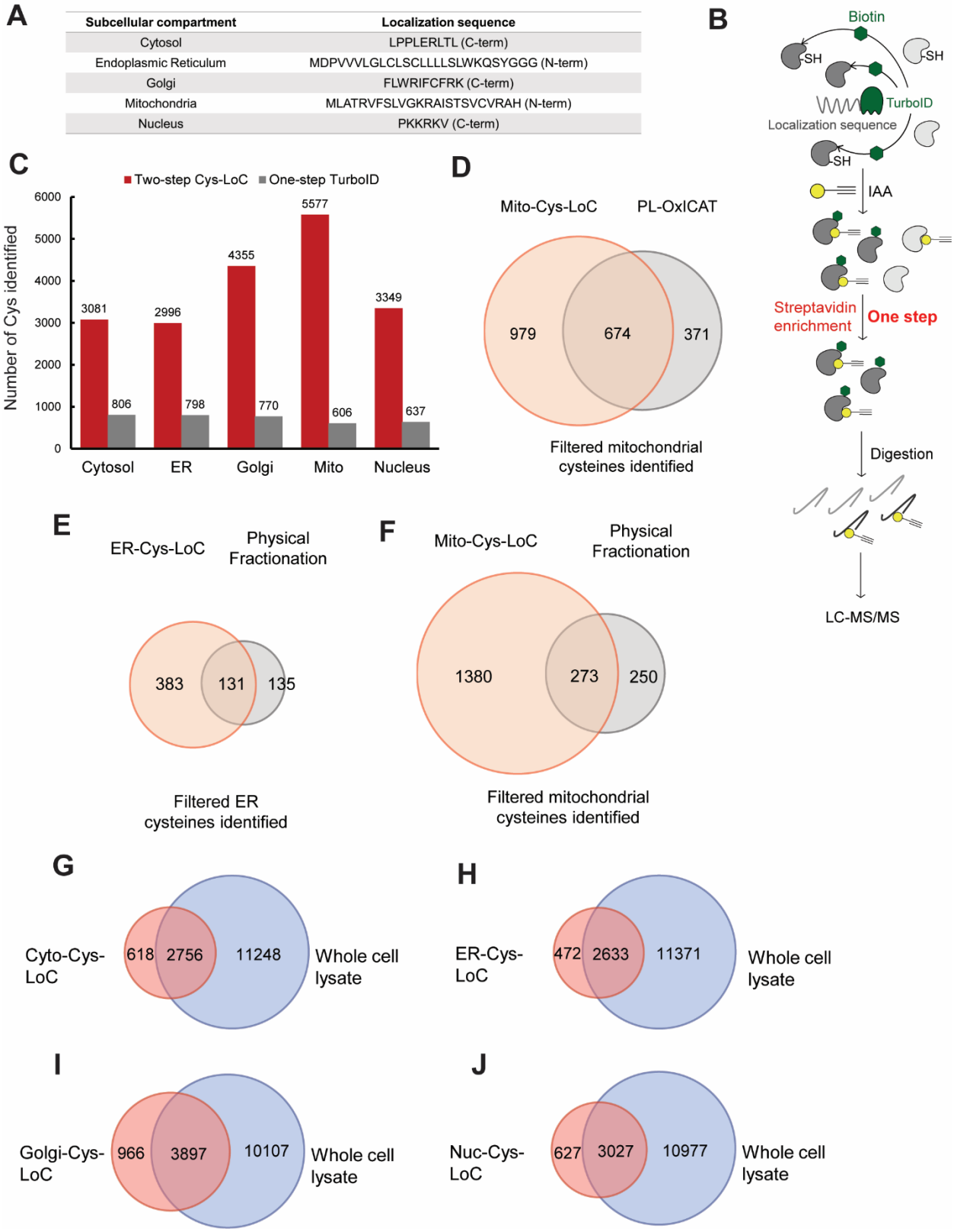

Figure S1. Establishment of Local Cysteine Capture (Cys-LoC) method. Related to Figure 1. A) Different localization sequence. **B)** Scheme of One-step TurboID. **C)** Number of cysteines

identified by Two-step Cys-LoC vs One-step TurboID in different subcellular compartments. Experiments were performed in singlicate in 293T cells. **D)** Comparison of the mitochondrial cysteines identified in this study to those in prior study with one-step proximity labeling[1]. **E-F)** Comparison of the cysteines identified in this study to those in other studies based on differential centrifugation fractionation[2,3]. **G-H)** Cysteines identified in different subcellular compartments with Cys-LoC. For panel G-H, experiments were performed in duplicate in HEK293T cells.

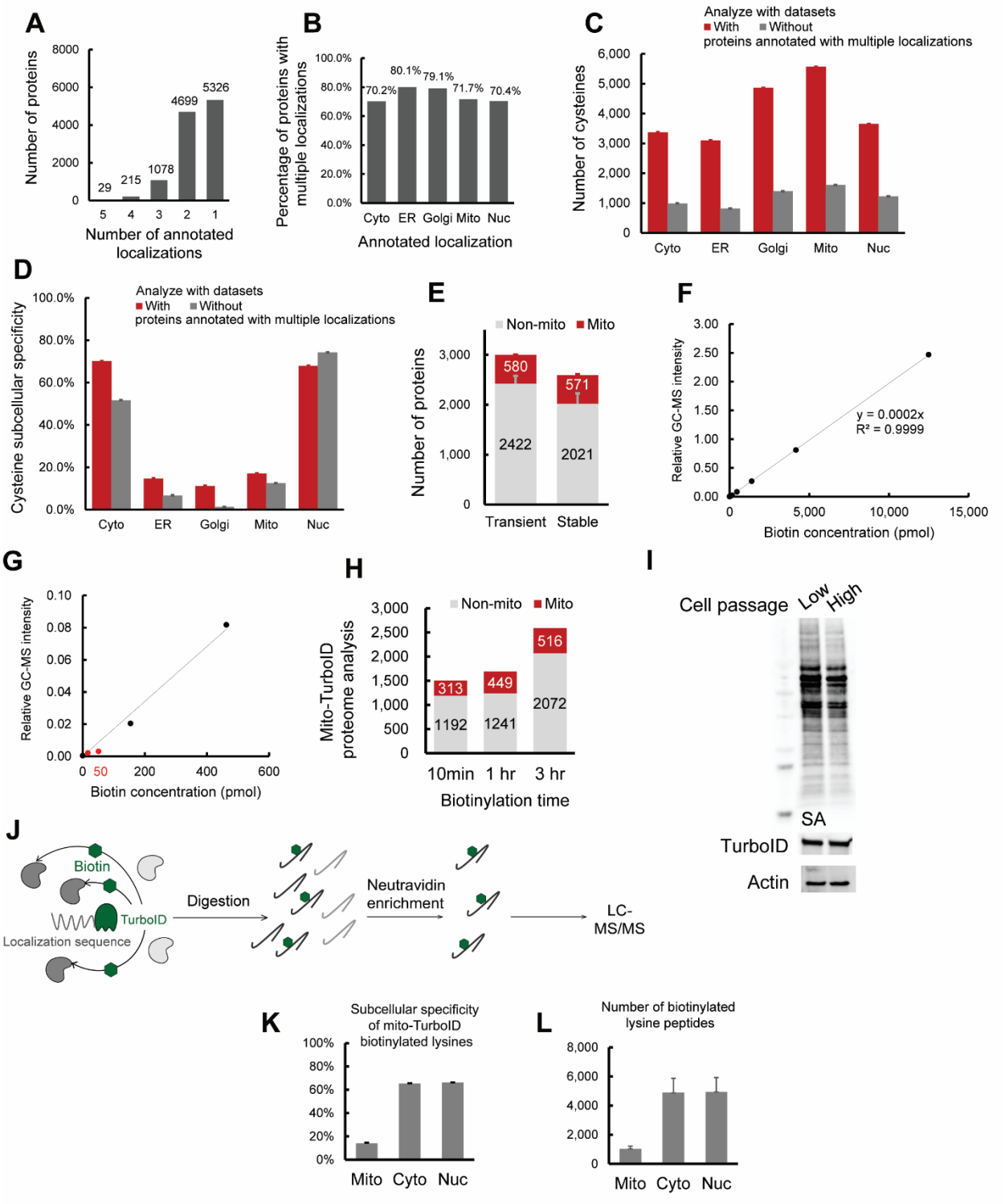

Figure S2. Pinpointing sources of non-compartment specific TurboID biotinylation. Related to Figure 2. A) Number of proteins by number of localization annotations. **B)** Percentage of proteins within each subcellular compartment containing greater than 1 annotated localization. **C)** Cysteines identified with Cys-LoC within proteins that are with and without multi-localization annotations. **D)** Compartment specificity analysis for Cys-LoC with dataset including multi-

localization proteins and for subset of dataset limited to proteins with localization restricted to a single compartment. **E)** Number of mitochondrial annotated proteins and non-mitochondrial annotated proteins identified with transiently or stably expressed mito-TurboID. **F-G)** Standard curve of biotin molecules detected with optimized GC-MS protocol. **H)** Number of mitochondrial annotated proteins and non-mitochondrial annotated proteins identified with mito-TurboID with biotinylation of 10 min or 1hr or 3hr. **I)** Biotinylation efficiency of mito-TurboID stably expressed in HEK293T cells < 10 passages (Low) or cells > 10 passages (High). **J)** Scheme of profiling lysines biotinylated by TurboID ligase. **K)** Subcellular specificity of mito-TurboID biotinylated lysines. **L)** Number of biotinylated lysine peptides annotated in different compartments enriched with mito-TurboID. For panel H, experiments were performed in singlicate in HEK293T cells. For panel C, D, E, F, G, K, L, experiments were performed in duplicate in HEK293T cells. Data in panel C, D, E, K, L are represented as mean ± SEM.

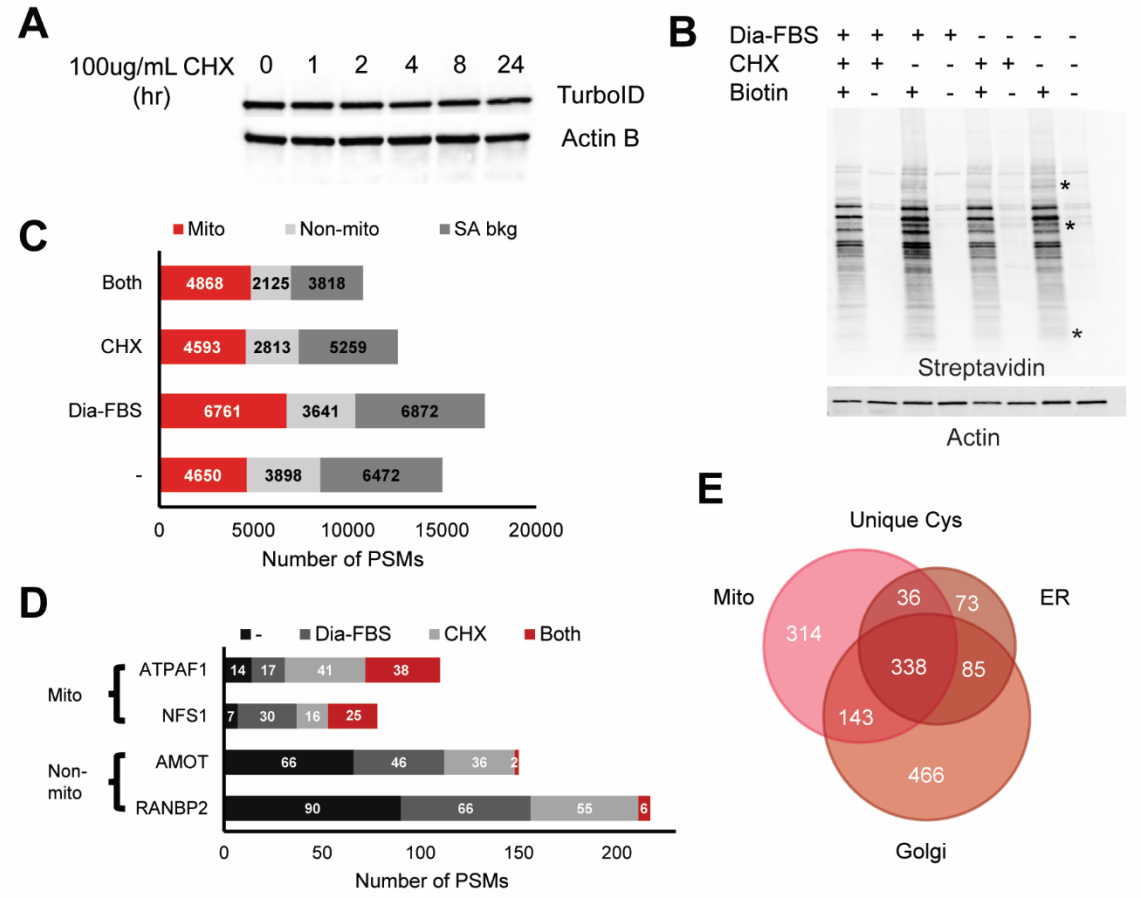

Figure S3. Translation arrest improves the subcellular specificity of proteins enriched by TurboID and cysteines captured by Cys-LoC. Related to Figure 3. A) Expression of TurboID upon treatment of the translational inhibitor CHX. **B)** Biotinylation of mito-TurboID with no treatment, with dialyzed FBS, with CHX treatment or with both. **C)** Proteome analysis of the proteins enriched with mito-TurboID with control condition, with dialyzed FBS, with CHX treatment or with both. **D)** Number of PSMs of representative mitochondrial proteins and non-mitochondrial proteins enriched with mito-TurboID for control condition, dialyzed FBS, CHX treatment or with both. **E)** Cysteines identified with optimized Cys-LoC targeting different subcellular compartments. Dialyzed FBS (Dia-FBS) treatment was 36 h and CHX treatment was 100 ug/mL for 6 h at 37 °C. For panel C, D, E, experiments were performed in triplicates in HEK293T cells.

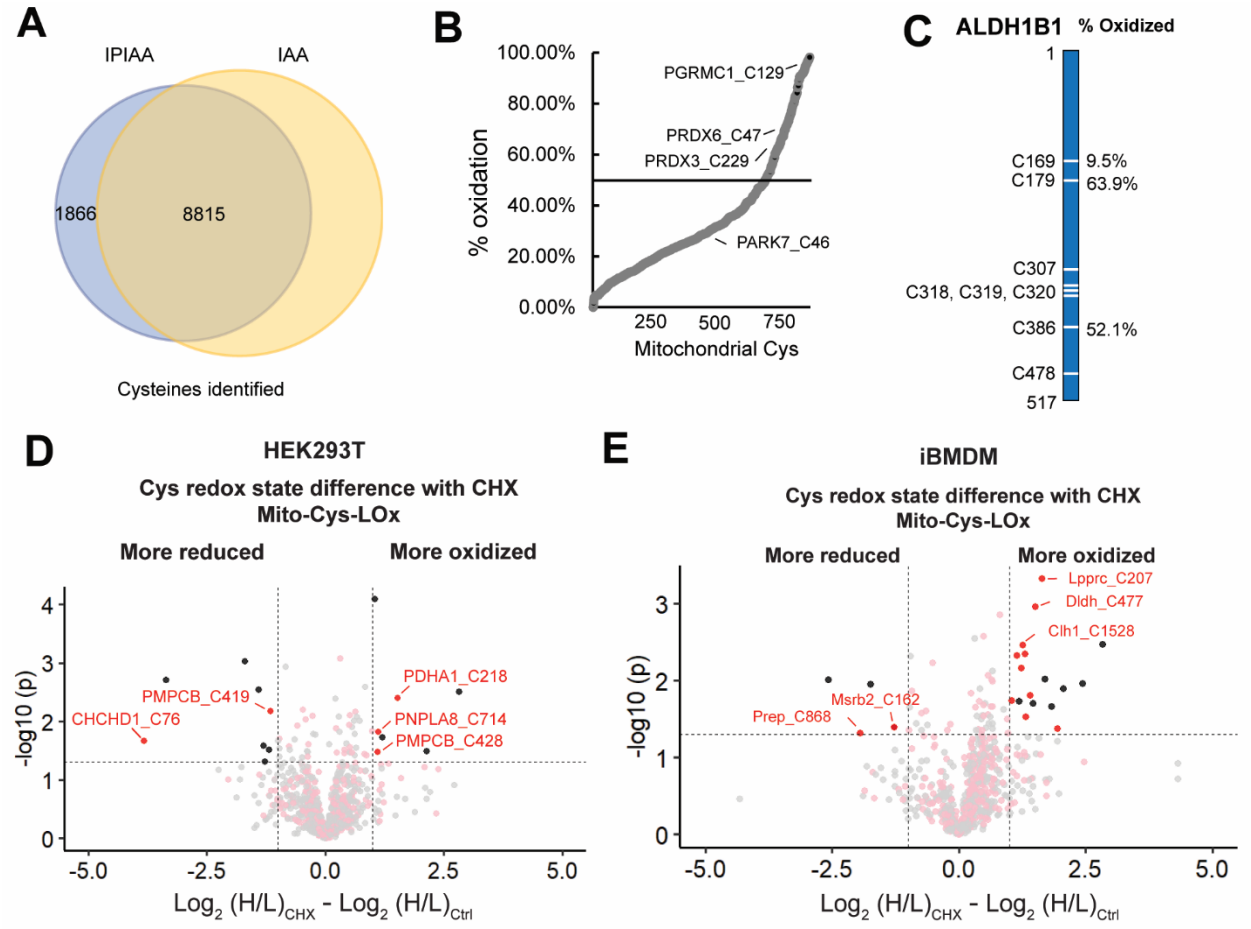

Figure S4. **Establishing the Local Cysteine Oxidation (Cys-LOx) method to analyze basal mitochondrial cysteine oxidation states. Related to Figure 4. A)** Venn diagram of cysteines captured and identified with IPIAA and IAA probes. **B)** Percentage oxidation states of mitochondrial cysteines identified with mito-Cys-LOx. **C)** Percentage oxidation states of cysteines quantified in exemplary mitochondrial proteins. **D)** Difference in redox states of cysteines quantified with Mito-Cys-LOx with or without dialyzed FBS and CHX treatment. **E)** Difference in redox states of cysteines quantified with Mito-Cys-LOx with or without dialyzed FBS and CHX treatment. Red dots indicate cysteines localized in mitochondria. Black dots indicate cysteins localized in organelles other than mitochondria. Dialyzed FBS (Dia-FBS) treatment was 36 h and CHX treatment was 100 ug/mL for 6 h at 37 °C. For panel B, C, D, experiments were performed in triplicates in HEK293T cells. For panel E, experiments were performed in triplicates in iBMDM cells.

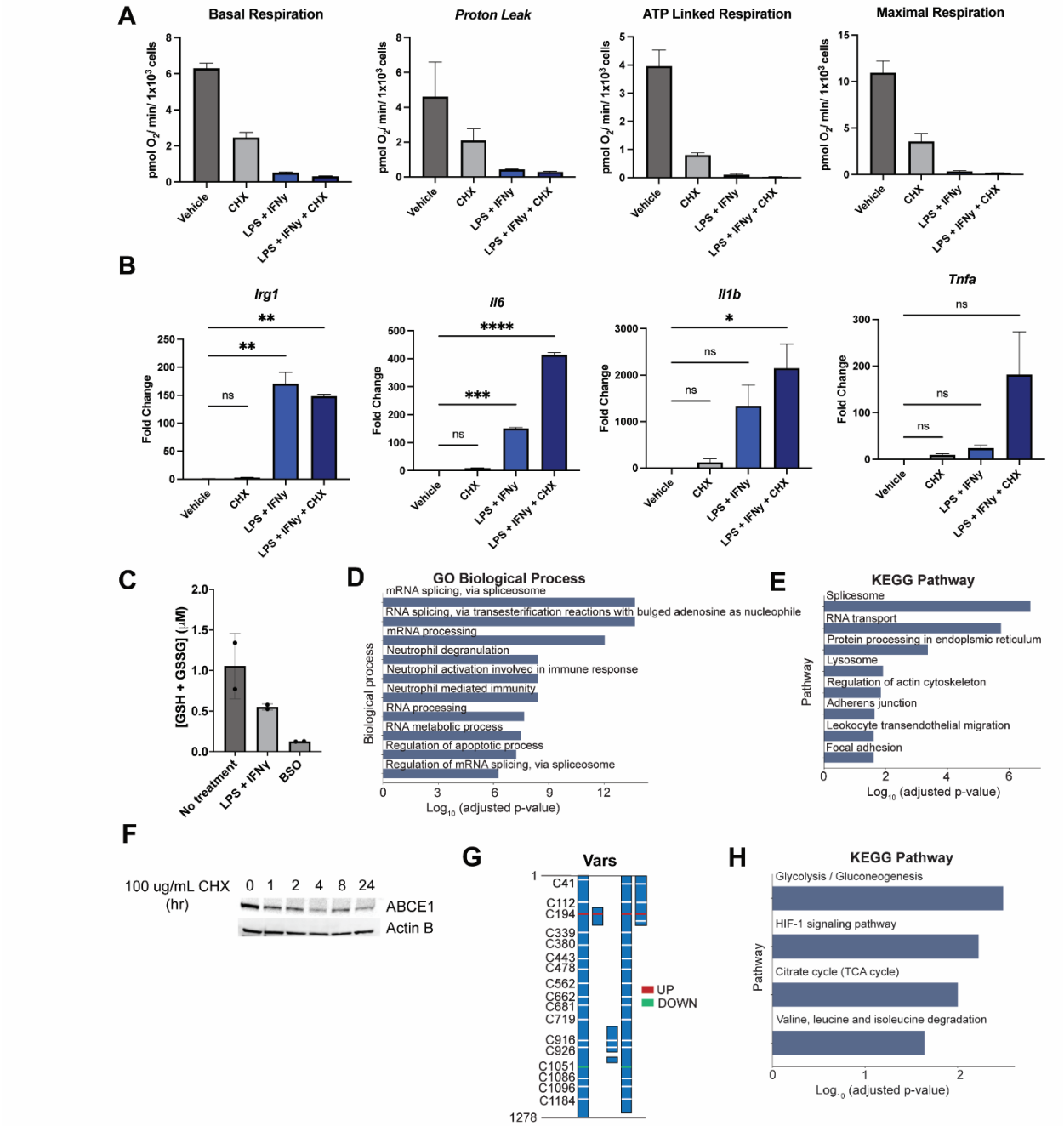

Figure S5. Cys-LOx outperforms SP3-Rox for quantification of LPS-induced changes of mitochondrial cysteine oxidation states. Related to Figure 5. A) Seahorse analysis of iBMDMs with control, LPS+IFNγ, CHX or both. **B)** qPCR analysis of LPS related genes with control, LPS+IFNγ, CHX or both. Statistical significance was calculated with unpaired Student's t-tests, * $p<0.05$, ** $p<0.01$, *** $p<0.005$. NS $p>0.05$. **C)** Amount of GSH detected in cells with or without LPS+IFNγ treatment. BSO was the negative control of the assay. **D)** GO biological process analysis of cysteines quantified with SP3-Rox that showed more reduced redox states upon LPS+IFNγ treatment. **E)** KEGG pathway analysis of cysteines quantified with SP3-Rox that showed more reduced redox states upon LPS+IFNγ treatment. **F)** Expression of ABCE1 upon treatment of translational inhibitor. **G)** Difference of redox states of cysteines quantified with SP3-

Rox with or without LPS+IFNγ treatment in exemplary proteins with different splice forms. **H)** KEGG pathway analysis of mitochondrial cysteines quantified with Mito-Cys-LOx that showed more oxidized redox states upon LPS+IFNγ treatment. Dialyzed FBS (Dia-FBS) treatment was 36 h, CHX treatment was 100 ug/mL for 6 h at 37 °C. LPS+IFNγ treatment was 100 ng/mL LPS and 20 ng/mL IFNγ for 24 h at 37 °C. For panel A, experiments were performed in 5 technical replicates in iBMDM cells. For panel B, C, experiments were performed in triplicates in iBMDM cells. For panel D, E, G, H, experiments were performed in triplicates in iBMDM cells with technical replicates. Data in panel A, B, C are represented as mean ± SEM.

Table S1. Conditions of Liquid-chromatography (LC). Related to STAR Methods

Parameter	Condition
Column	100 µM ID fused silica capillary packed in-house with bulk C18 reversed phase resin (particle size, 1.9 µm; pore size, 100 Å; Dr. Maisch GmbH)
Mobile phase	Buffer A: water with 3% DMSO and 0.1% formic acid Buffer B: 80% acetonitrile with 3% DMSO and 0.1% formic acid
Gradient and flow rate	0 – 5 min, 3 – 10% B, 300 nL/min 5 – 64 min, 10 - 50% B, 220 nL/min 64 – 70 min, 40 - 95% B, 250 nL/min
Run time	70 minutes
Injection volume	5 uL

Table S2. Files in Proteomics Identification Database (PRIDE) datasets. Related to STAR Methods.

Figure	File name	Experiment
1 (HEK 293T)	2020-10-05-KB-70min_FAIMS_3cv_-35_-45_-55_OTOT_SY41-1 2020-10-05-KB-70min_FAIMS_3cv_-35_-45_-55_OTOT_SY41-2	Cys-Whole lysate
	2022-08-25-KB-noFAIMS-SY87-1 2022-03-24-KB-SY87-1	Cyto-Cys-LoC
	2022-08-25-KB-noFAIMS-SY87-3 2022-03-24-KB-SY87-3	ER-Cys-LoC
	2022-08-25-KB-noFAIMS-SY87-4 2022-03-24-KB-SY87-4	Golgi-Cys-LoC
	2022-08-25-KB-noFAIMS-SY93-T500 2022-05-15-KB-nofaims-SY91-5a	Mito-Cys-LoC
	2022-08-25-KB-noFAIMS-SY87-5 2022-03-24-KB-SY87-5	Nuc-Cys-LoC
2 (HEK 293T)	2022-06-14-KB-NoFAIMS-standard 2022-05-14-KB-nofaims-standard	Whole lysate
	2022-05-03-KB-SY91-ZT-1a 2022-05-03-KB-SY91-ZT-1b	Cyto-TurboID
	2022-05-03-KB-SY91-ZT-3a 2022-05-03-KB-SY91-ZT-3b	ER-TurboID
	2022-05-03-KB-SY91-ZT-4a 2022-05-03-KB-SY91-ZT-4b	Golgi-TurboID
	2022-05-03-KB-SY91-ZT-5a 2022-05-03-KB-SY91-ZT-5b	Mito-TurboID
	2022-05-03-KB-SY91-ZT-6a 2022-05-03-KB-SY91-ZT-bb	Nuc-TurboID
3 (HEK 293T)	2022-08-10-noFAIMS-SY98-1-1 2022-08-10-noFAIMS-SY98-1-2 2022-08-10-noFAIMS-SY98-1-3	Ctrl Mito-TurboID
	2022-08-11-KB-noFAIMS-SY98-3-1 2022-08-11-KB-noFAIMS-SY98-3-2 2022-08-11-KB-noFAIMS-SY98-3-3	Dia-FBS Mito-TurboID

	2022-08-11-KB-noFAIMS-SY98-4-1 2022-08-11-KB-noFAIMS-SY98-4-2 2022-08-11-KB-noFAIMS-SY98-4-3	CHX Mito-TurboID
	2022-08-08-noFAIMS-SY98-5-1 2022-08-08-noFAIMS-SY98-5-2 2022-08-08-noFAIMS-SY98-5-3	Dia-FBS + CHX Mito-TurboID
	2022-08-20-KB-noFAIMS-SY99-1-1 2022-08-20-KB-noFAIMS-SY99-1-2 2022-08-20-KB-noFAIMS-SY99-1-3	Ctrl Mito-Cys-LoC
	2022-08-20-KB-noFAIMS-SY99-2-1 2022-08-20-KB-noFAIMS-SY99-2-2 2022-08-20-KB-noFAIMS-SY99-2-3	Dia-FBS + CHX Mito-Cys-LoC
	2022-08-20-KB-noFAIMS-SY99-5-1 2022-08-20-KB-noFAIMS-SY99-5-2 2022-08-20-KB-noFAIMS-SY99-5-3	Dia-FBS + CHX ER-Cys-LoC
	2022-08-20-KB-noFAIMS-SY99-6-1 2022-08-20-KB-noFAIMS-SY99-6-2 2022-08-20-KB-noFAIMS-SY99-6-3	Dia-FBS + CHX Golgi-Cys-LoC
4 (iBMDM)	2022-10-07-KB-SY104-1-1 2022-10-07-KB-SY104-1-2 2022-10-07-KB-SY104-1-3	Ctrl Mito-Cys-LOx
	2022-10-07-KB-SY104-2-1 2022-10-07-KB-SY104-2-2 2022-10-07-KB-SY104-2-3	Dia-FBS + CHX Mito-Cys-LOx
5 (iBMDM)	2022-10-07-KB-AJ-2stepredox-NT-1 2022-10-07-KB-AJ-2stepredox-NT-2 2022-10-07-KB-AJ-2stepredox-NT-3 2022-11-23-KB-AJ-2stepredox-NT-1-rerun 2022-11-23-KB-AJ-2stepredox-NT-2-rerun 2022-11-23-KB-AJ-2stepredox-NT-3-rerun	Ctrl Mito-Cys-LOx
	2022-10-07-KB-AJ-2stepredox-LPS-1 2022-10-07-KB-AJ-2stepredox-LPS-2 2022-10-07-KB-AJ-2stepredox-LPS-3 2022-11-23-KB-AJ-2stepredox-LPS-1-rerun 2022-11-23-KB-AJ-2stepredox-LPS-2-rerun 2022-11-23-KB-AJ-2stepredox-LPS-3-rerun	LPS Mito-Cys-LOx
	2022-11-19-KB-noFAIMS-MV-SY-B16-mito-turboID-NT-2 2022-11-19-KB-noFAIMS-MV-SY-B16-mito-turboID-NT-4 2022-11-19-KB-noFAIMS-MV-SY-B16-mito-turboID-NT-6 2022-11-23-KB-noFAIMS-MV-SY-B16-mito-turboID-NT-2-rerun 2022-11-23-KB-noFAIMS-MV-SY-B16-mito-turboID-NT-4-rerun	Ctrl SP3-Rox

	2022-11-23-KB-noFAIMS-MV-SY-B16-mito-turboID-NT-6-rerun	
	2022-11-19-KB-noFAIMS-MV-SY-B16-mito-turboID-LPS-1 2022-11-19-KB-noFAIMS-MV-SY-B16-mito-turboID-LPS-3 2022-11-19-KB-noFAIMS-MV-SY-B16-mito-turboID-LPS-5 2022-11-23-KB-noFAIMS-MV-SY-B16-mito-turboID-LPS-1-rerun 2022-11-23-KB-noFAIMS-MV-SY-B16-mito-turboID-LPS-3-rerun 2022-11-23-KB-noFAIMS-MV-SY-B16-mito-turboID-LPS-5-rerun	LPS SP3-Rox

References

[S1] Kisty, E.A., Falco, J.A., and Weerapana, E. (2023). Redox proteomics combined with proximity labeling enables monitoring of localized cysteine oxidation in cells. Cell Chem. Biol. *30*, 321-336.e6. 10.1016/j.chembiol.2023.02.006.

[S2] Bak, D.W., Pizzagalli, M.D., and Weerapana, E. (2017). Identifying Functional Cysteine Residues in the Mitochondria. ACS Chem. Biol. *12*, 947–957. 10.1021/acschembio.6b01074.

[S3] Bechtel, T.J., Li, C., Kisty, E.A., Maurais, A.J., and Weerapana, E. (2020). Profiling Cysteine Reactivity and Oxidation in the Endoplasmic Reticulum. ACS Chem. Biol. *15*, 543–553. 10.1021/acschembio.9b01014.